# Identification of Hub Genes of Mesio Temporal Lobe Epilepsy and Prognostic Biomarkers of Brain Low-grade Gliomas Based on Bioinformatics Analysis

Jian Xu[1] (iD), Mingqiang Sun[2], Yuanyuan Wang[3], Anmu Xie[4], and Jian Gao[3]

## Abstract

Mesio temporal lobe epilepsy (MTLE) syndrome is the most common form of intractable epilepsies. Meanwhile, seizures are common in patients with cancer as a consequence of brain tumors, including brain low-grade gliomas (LGG). However, the underlying molecular mechanisms of MTLE remain poorly understood. Also, the relationship between MTLE and LGG needs our attention. In this study, we aimed to investigate the hub genes and potential mechanism in MTLE, and the relationship between MTLE and LGG, the gene expression profiles (GSE88992) were downloaded from the Gene Expression Omnibus (GEO) database. Difference analysis for MTLE versus control groups under the three time points was conducted to select the differentially expressed genes (DEGs). Time series clustering analysis was used to select the trend genes. Then a series of bioinformatics analyses including functional enrichment analysis, protein–protein interaction (PPI) network and module analyses, and transcription factor (TF) and miRNA prediction were performed. Also, the overall survival analysis and expression of hub genes in LGG were performed using UALCAN from TCGA database. At 6 h, there were 351 upregulated and 80 downregulated DEGs. At 12 h, there were 499 upregulated and 231 downregulated DEGs. Additionally, 532 upregulated and 402 downregulated DEGs were obtained at 24 h. After time series clustering analysis of the DEGs, we obtained 323 uptrend and 248 downtrend genes. We identified 10 key genes with higher degrees, including C3, TIMP1, PENK, CKAP4, etc. Five PPI modules were identified by MCODE. TF analysis predicted four TFs: JUN, STAT3, NR4A2, and Myc. A total of 26,834 miRNA–mRNA pairs were predicted. Moreover, survival analysis of UALCAN suggested that C3, TIMP1, PENK, GNG2, CKAP4, TNC, JUN, STAT3, NR4A2, and Myc can be potential biomarkers for the prognosis of LGG. In summary, DEGs and hub genes were identified in the present study, which provides novel insight into the development of MTLE.

## Keywords

mesio temporal lobe epilepsy (MTLE), low-grade gliomas (LGG), bioinformatics, biomarker, time series clustering analysis

[1] Department of Neurology, The Affiliated Hospital of Qingdao University, Qingdao, China
[2] Department of Clinical Lab, Maternal and Child Health Hospital of Weifang Medical University, Weifang, Shandong, China
[3] Department of Pediatric, Maternal and Child Health Hospital of Weifang Medical University, Weifang, Shandong, China
[4] Department of Neurology, The Affiliated Hospital of Qingdao University, Qingdao, China

**Corresponding Authors:**
Jian Xu, Department of Neurology, The Affiliated Hospital of Qingdao University, Qingdao 266000, China.
Email: ydukongjian@163.com;

Jian Gao, Department of Pediatric, Maternal and Child Health Hospital of Weifang Medical University, Weifang, Shandong 261011, China.
Email: gaojian1650@126.com;

Anmu Xie, Department of Neurology, The Affiliated Hospital of Qingdao University, Qingdao 266000, China.
Email: xieanmu@163.com

## Introduction

Epilepsy is a serious neurological disorder, which is characterized by spontaneous recurrent seizures and a high incidence of comorbid health conditions[1]. Mesio temporal lobe epilepsy (MTLE) is one of the most common forms of intractable epilepsies. It has been reported that all patients with MTLE have experienced one or more triggering disorders, such as head trauma, intracerebral infections, complex febrile seizures, or ischemic episodes in early childhood[2,3]. Currently, significant signs of progress have been made in understanding the disease processes in the epilepsies. Many genetic variants related to common and rare epilepsies have been reported[4-6]. However, there is still no accurate biomarker or effective therapeutic target for epileptogenesis.

To search for biomarkers for MTLE, RNA-seq and microarray methods have been used to study representative animal models of MTLE[7-9]. Nevertheless, some of these studies induce a status epilepticus for several hours in the rat through systemic injections of kainite[10], which leads to bilateral lesions of different brain structures, and systemic convulsions. The two features may be confused with those observed in MTLE patients[11]. Additionally, in some studies, the brain samples were collected from animals that were experiencing seizures, either during the status epilepticus or later[12], which raised the concern that the observed changes may be a consequence of seizures.

To avoid the concerns above, Kalozoumi et al.[13] recently established an MTLE mouse model by intra-hippocampal microinjection of kainate. They then conducted whole-genome expression analyses of the hippocampus at 6, 12, and 24 h of injection to depict the molecular changes in the early stages of epileptogenesis. Although some key regulators of MTLE, such as vimentin, cytochrome B-245 alpha chain, and cytochrome B-245 beta chain have been identified, the understanding of molecular mechanisms underlying MTLE is still limited using the integrated bioinformatics methods, and multidimensional evaluation of the complex pathogenesis in MTLE is still required.

Seizures are the presenting symptom in approximately one-third of patients with brain tumors, including both primary and metastatic tumors. During their illness, many patients who have cancer experience seizures, with the incidence varying according to the type of tumor. Low-grade gliomas (LGG) ranked third among them[14]. Although LGG (astrocytomas, oligodendrogliomas, and oligoastrocytomas) are considered relatively benign, well-differentiated tumors and have 5-year survival rates of 59.9%, approximately 70% of LGG patients develop GBM within 5–10 years[15]. Therefore, it is necessary to further understand the relationship between epilepsy and LGG by understanding the molecular basis of epilepsy, which is an important step in defining new biomarkers and therapeutic strategies of MTLE and LGG.

Thus, the present study aimed to explore possible molecular mechanisms and biomarkers of MTLE and the relationship between the MTLE and LGG. We first selected the candidate genes from the Gene Expression Omnibus (GEO) dataset (accession number: GSE88992) deposited by Kalozoumi et al.[13] through time series clustering analysis. Then a series of bioinformatics analyses including functional enrichment analysis, protein–protein interaction (PPI) network and module analyses, and transcription factor (TF) and miRNA prediction were performed. We further performed the expression of the key genes and survival analysis by using UALCAN data.

## Materials and Methods

### Microarray Data

Dataset GSE88992 (species: *Mus musculus*) were downloaded from the NCBI GEO[16] database. The dataset contains 17 samples obtained from three time points: 6, 12, and 24 h. For each time point, intrahippocampal microinjection of kainate (1 nmol/50 nl) and saline (control) was performed. All samples were detected using the [Mouse430_2] Affymetrix Mouse Genome 430 2.0 Array platform.

### Differentially Expressed Genes Screening

The probe expression matrix file GSE88992 series matrix.txt was downloaded from the GEO database. The probes were annotated with the annotation file to remove the probe that did not map the gene symbol. If different probes mapped to the same gene, the mean value of different probes was taken as the final expression value of this gene.

Using the classical Bayes method provided by the limma package[17] (version 3.10.3), difference analysis for kainate versus control groups under the three time points was conducted to select the differentially expressed genes (DEGs). The $P$-value and log fold change (FC) value of all genes were obtained. Then Benjamini and Hochberg method was used for multiple test correction, obtaining the adjusted $P$-value (adj.p.value). The thresholds for DEGs screening were set as follows: adj.p.value < 0.05 and |logFC| > 1.

### Time Series Clustering Analysis

The union sets of differentially expressed up- or downregulated genes at all time points were clustered by using Short Time-series Expression Miner (STEM)[18] v1.3.11. In detail, the average expression value of each gene under every time point was calculated as input, and the control group considered as 0 h. Then based on the software default parameters, the DEGs set that presented an upward or downward trend over time was searched ($P$-value < 0.001 was defaulted to significant in STEM). These genes were considered to be gene clusters that varied significantly with kainate treatment time.

## Functional and Pathway Enrichment Analysis of Trend Genes

The DEGs set that presented an up- or downtrend over time were subjected to Gene Ontology (GO)[19] function and KEGG[20] pathway enrichment analyses using the DAVID database (version 6.8). Significance thresholds were set as $P < 0.05$ and enrichment number (count) $\geq 5$.

## PPI Network Analysis

The interaction of these DEGs was analyzed using STRING (https://string-db.org/)[21] (version: 10.0) database. The input gene set was the trend gene obtained above, and the species was *M. musculus*. PPI score was set to 0.9 (highest confidence), and the protein nodes should be included in the up- and downregulated DEGs. Furthermore, Cytoscape software[22] (version 3.4.0) was used for network construction. The network node connectivity degree was analyzed using CytoNCA plugin[23] (version 2.1.6) (parameter: without weight). The hub genes (Degree > 10) involved in the PPI network were selected through degree ranking.

## PPI Module Analysis

In the PPI network, the functional modules were identified by clustering analysis. MCODE plugin[24] was used to analyze PPI network module, and MCODE score $\geq 5$ (parameters: Node Score Cutoff = 0.2, Degree Cutoff = 2, k-core = 2, max. depth = 100). Then, the obtained modules were subjected to KEGG pathway analysis using clusterProfiler[25] (version 3.8.1). The pathways with BH adjusted adj.p.value < 0.05 were considered as significant enrichment results, which were displayed in bubble charts.

## TF Regulatory Network Analysis

TRRUST (version 2) contains 8444 regulatory interactions for 800 TFs in humans as well as 6552 TF–target interactions for 828 mouse TFs[26]. In this study, the TFs for up- or downtrend genes were predicted using TRRUST database (species: *M. musculus*). Following that, the TFs that differentially expressed in at least one point time and the TF-target regulatory relations with $P$-value < 0.05 were selected to build the TF-target regulatory network.

## Upstream miRNA Prediction

miRWalk2.0[27] is a comprehensive database, which provides the largest available set of predicted and experimentally validated miRNA-target interactions. Additionally, it not only records miRNA binding sites in the complete sequence of genes but also compared this information with the binding sites of 12 existing miRNA-target prediction programs: miR-Map, miRWalk, miRNAMap, MicroT4, TargetScan, RNA-hybrid, PICTAR2, miRBridge, PITA, miRanda, miRDB, and RNA22. Now we used the predicted Target Module in

miRWalk 2.0 to predict the miRNAs for the trend genes (species: *M. musculus*). The miRNAs that simultaneously appeared in miRWalk, Microt4, miRanda, RNA22, and Targetscan databases were selected as the upstream regulatory molecules of the corresponding genes. After obtaining miRNA–mRNA relation pairs, miRNAs with the number of target genes in the TOP20 were selected for miRNA-target network construction.

## Functional Pathway Enrichment Analysis of miRNAs

The KEGG pathway enrichment analysis of the corresponding target genes of the miRNA was carried out using clusterProfiler, and the pathways with adj.p.value < 0.05 were selected as the pathway of miRNAs. The results were displayed in bubble charts.

## Expression and Survival Analysis of DEGs in LGG Between the Grade 2 and Grade 3

Kaplan–Meier curve was used to evaluate the effects of DEGs on the overall survival of LGG patients. According to the median gene expression levels between the LGG-Grade 2 (moderately differentiated) and LGG-Grade 3 (poorly differentiated), LGG patients were classified into high and low expression groups. The difference between high or low expression group was assessed by $P$-value. $P < 0.05$ was regarded as significant. The correlation between gene expression and clinical relevance was analyzed using UALCAN (https://ualcan.path.uab.edu/index.html) online dataset (Chandrashekar et al., 2017), which is a user-friendly, interactive web resource for the analysis of cancer transcriptome data.

## Quantitative Real-time Polymerase Chain Reaction Analysis

To confirm the microarray results, some DEGs were confirmed by quantitative real-time polymerase chain reaction (qRT-PCR) analysis. According to the previously described methods[13], 10 C57Bl/ 6 J mice (KA group: $n = 5$ and control group: $n = 5$) were selected randomly from each group and made the epileptic mouse model. After KA induction, hippocampus isolation, and RNA extraction, cDNA was prepared using the RevertAid™ First Strand cDNA Synthesis Kit (Thermo Fisher, Agawam, MA, USA). By employing the Real Master mix (SYBR Green) Kit (Tiangen, Beijing, China) and a LightCycler (Roche Diagnostics, Bremen, Germany), qRT-PCR was performed following the manufacturer's protocols. Single PCR products were further verified by melting curve analysis. Note that mice β-actin was always amplified in parallel with the representative genes. The relative expression ratio was determined by the formula $2^{-\triangle\triangle ct}$ method.
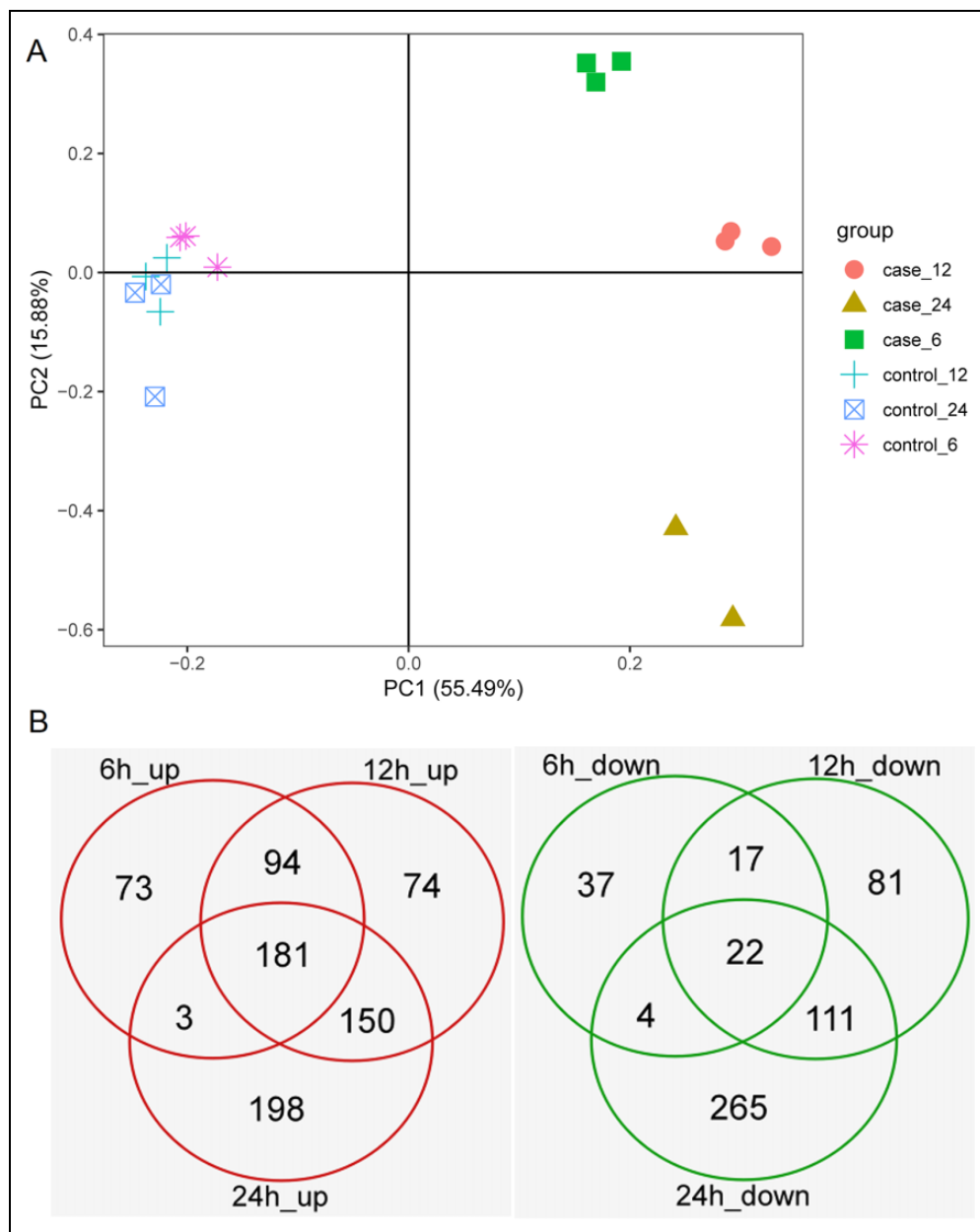
**Fig. 1.** Differentially expressed genes analysis. (A) Principal component analysis for samples. (B) Venn plots of up- and downregulated gene at each time point.

### Statistics

Statistical significance of differences between groups was assessed using Student's *t* tests. Throughout the text, summary data were presented as mean $\pm$ standard error of the mean.

## Results

### Differential Expression Analysis

Principal component analysis (PCA) showed that all eight samples under the different time points of the kainite (case) group were categorized into three main distinct clusters. Meanwhile, all nine samples of the control group were clustered together (Fig. 1A). The PCA result is consistent with our expectations.

The DEGs between kainate and control groups at each time point were identified by using the limma package. At 6 h, there were 351 upregulated and 80 downregulated DEGs. At 12 h, there were 499 upregulated and 231 downregulated DEGs. Additionally, 532 upregulated and 402 downregulated DEGs were obtained at 24 h. Interestingly, we found that the number of DEGs increases with the increase of treatment time, and upregulated and downregulated DEGs appear to follow the same pattern. Finally, a total of 773 upregulated and 537 downregulated DEGs were obtained at each time point through the Venn diagram (Fig. 1B, Supplemental Tables S1 and S2).
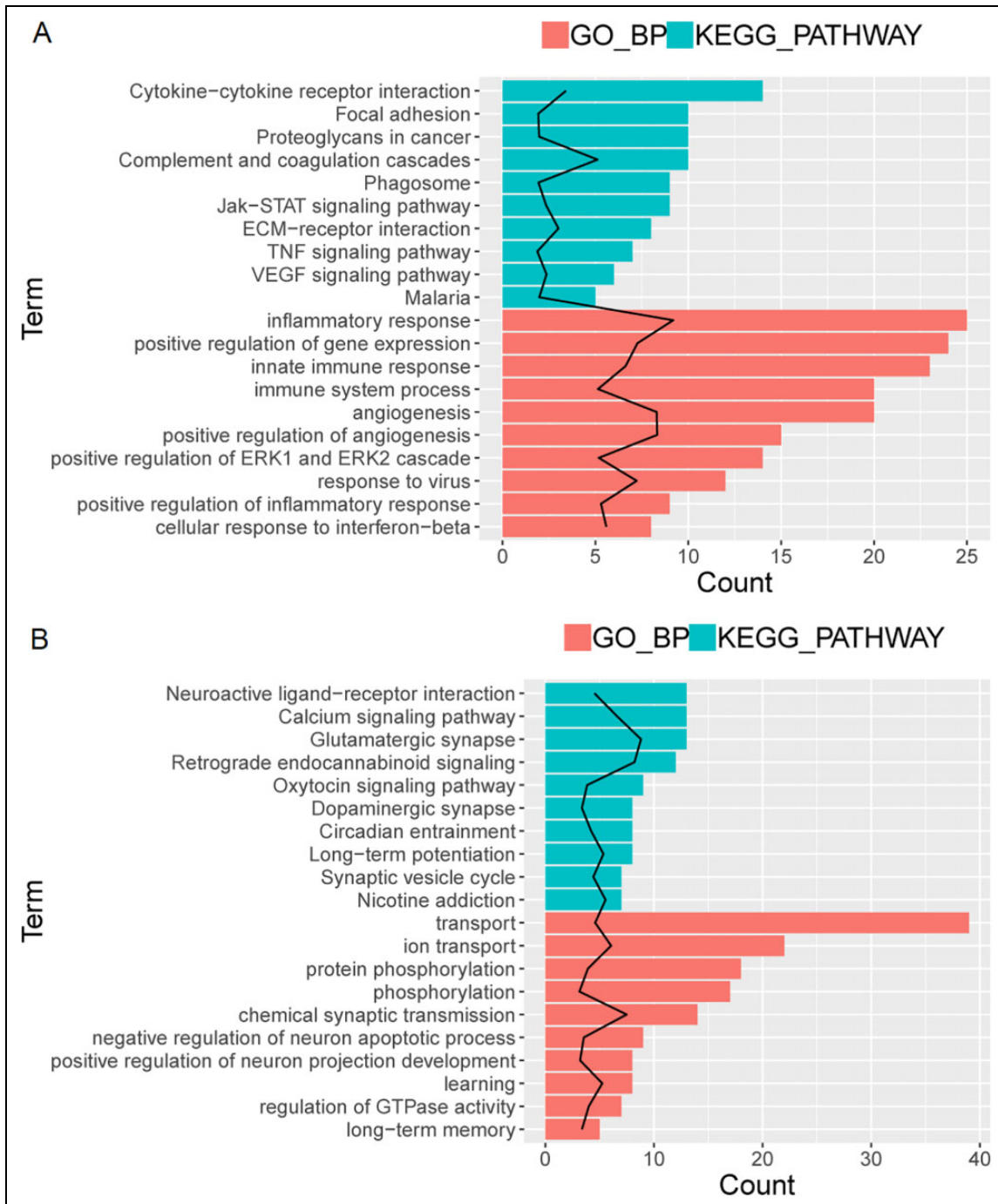
**Fig. 2.** STEM time series clustering analysis. The black line represents the overall trend, the number in the upper left corner represents the cluster number, the number in the lower left corner represents P-value, and the colored one represents the significant gene cluster (P-value < 0.001). STEM: Short Time-series Expression Miner.

**Fig. 3.** GO function and KEGG pathway for trend DEGs: uptrend genes (A) and downtrend genes (B). The black line represents −log10 (*P*-value), red represents GO BP, green represents KEGG pathway, and the length of the bar represents the number of enriched genes. BP: biological processes; DEGs: differentially expressed genes; GO: Gene Ontology.

## Time Series Clustering Analysis

From a biological point of view, genes with similar expression patterns may have common characteristics, such as being regulated by a gene at the same time or having similar biological functions. According to the threshold described in the method, a total of 11 significant gene clusters were obtained, as shown in Fig. 2. The clusters 42, 48, 40, and 29 were integrated as gene clusters with increased expression over time, including 323 genes, and clusters 9, 11, and 1 were integrated as gene clusters with decreased expression over time, containing 248 genes (Supplemental Table S3). These trend DEGs were considered to be gene clusters that changed significantly with the treatment time of kainate and were associated with the development of MTLE.
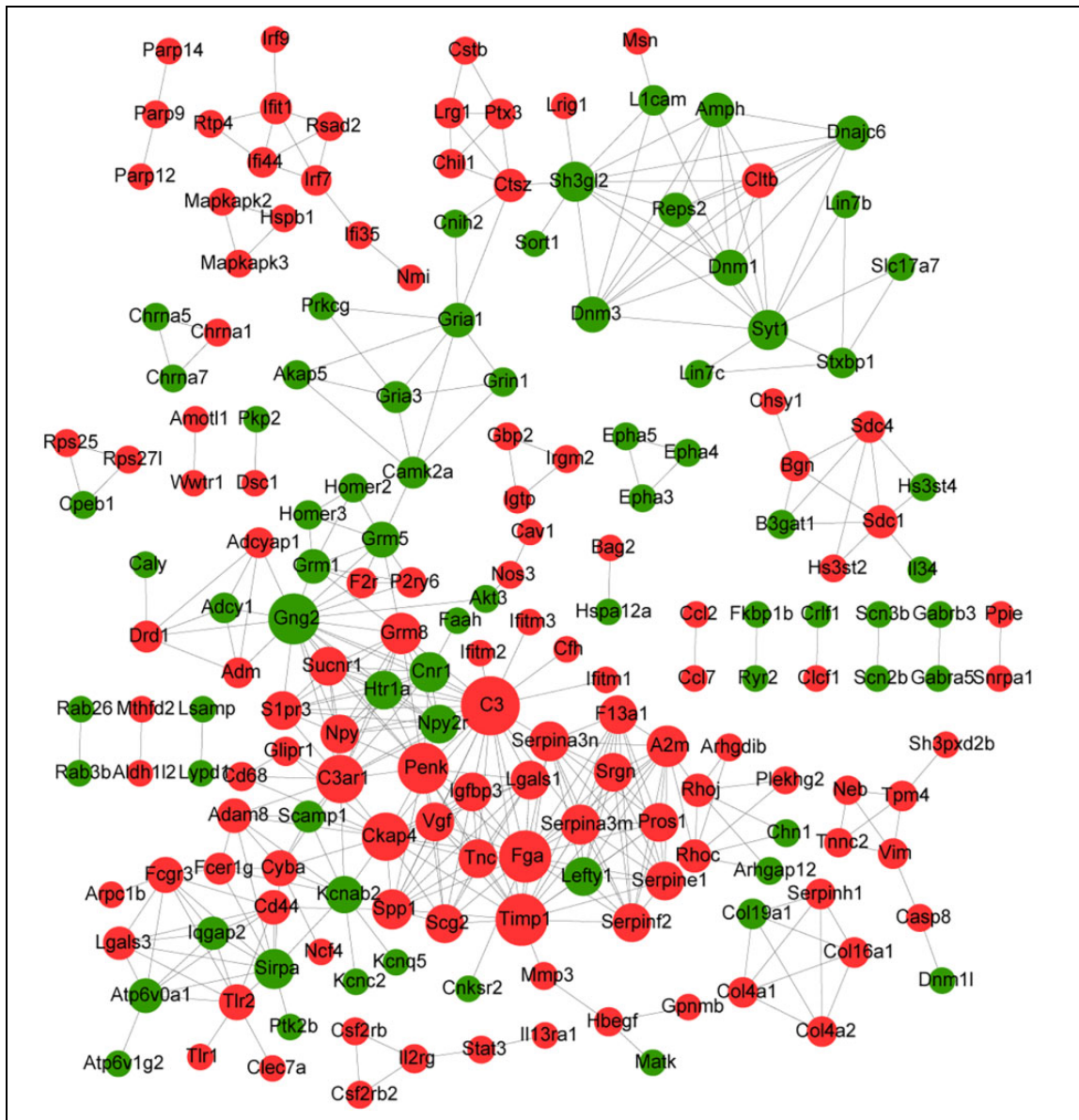
**Fig. 4.** PPI network analysis of trend DEGs. PPI network corresponding to up- and downtrend genes. The red node represents the uptrend gene, the green node represents the downtrend gene, and the node size represents the degree. DEGs: differentially expressed genes; PPI: protein–protein interaction.

## Functional and Pathway Enrichment Analyses of Trend Genes

To investigate the biological classification and KEGG pathway enrichment analyses of DEGs, the up- or downtrend DEGs of GO function were identified using DAVID (Supplemental Table S4). The cut-off criterion was set as $P < 0.05$. Top 10 changes of up- and downtrend DEGs in biological processes (BP) were significantly enriched in the inflammatory response, innate immune response, angiogenesis (Fig. 3A bottom), ion transport, chemical synaptic transmission, and neuron apoptotic process (Fig. 4B bottom).

The top 10 enriched KEGG pathways of up- and downtrend DEGs were abundant in cytokine–cytokine receptor interaction, jak-stat signaling pathway, TNF signaling pathway (Fig. 3A top), neuroactive ligand–receptor interaction, calcium signaling pathway, and glutamatergic synapse (Fig. 4B top). These significantly enriched GO terms and pathways will help us to understand key molecules in the development of MTLE.

## PPI Network Construction and Module Analysis

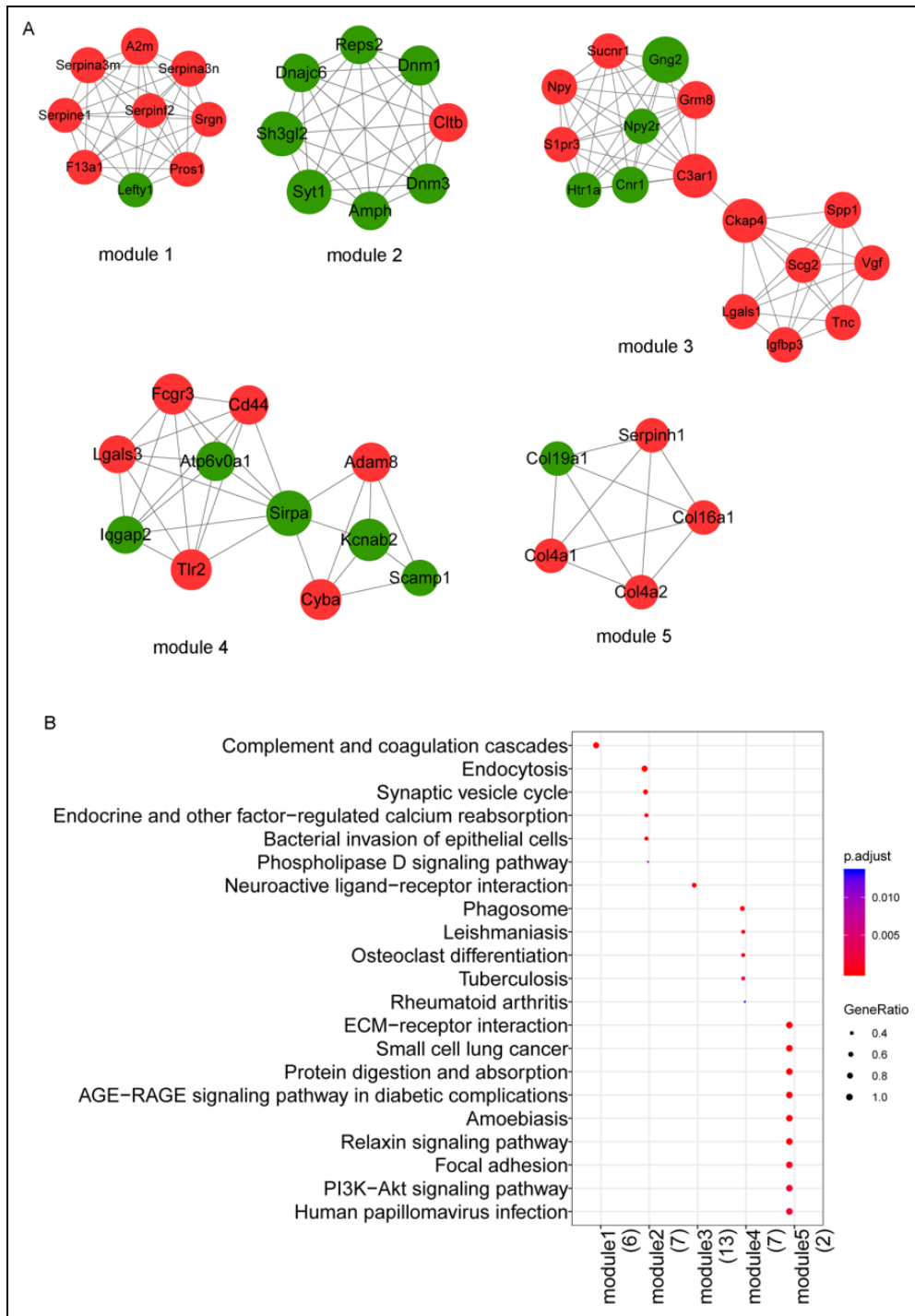To further investigate the interaction among the 571 up- and downtrend DEGs, a PPI network was constructed from

**Fig. 5.** PPI module analysis. (A) Subnetwork module of the protein–protein interaction network. The red node represents the uptrend gene, and the green node represents the downtrend gene. (B) Pathway analysis results of the subnetwork module. Color from blue to red indicates the decrease of adjusted *P*-value, and bubble size indicates the proportion of the number of enriched genes in the number of module genes annotated to KEGG pathway. PPI: protein–protein interaction.

STRING to elucidate PPI (Fig. 4). Analysis of the connectivity degrees of nodes in the network showed that the connectivity degrees of most nodes were small (less than 10) and only a few nodes had large degrees (more than 10), which conformed to the characteristics of PPI network, that is, only a few genes play an important role in the whole network. Genes with degrees greater than 10, including complement C3 (C3), fibrinogen alpha chain (FGA), TIMP metallopeptidase inhibitor 1
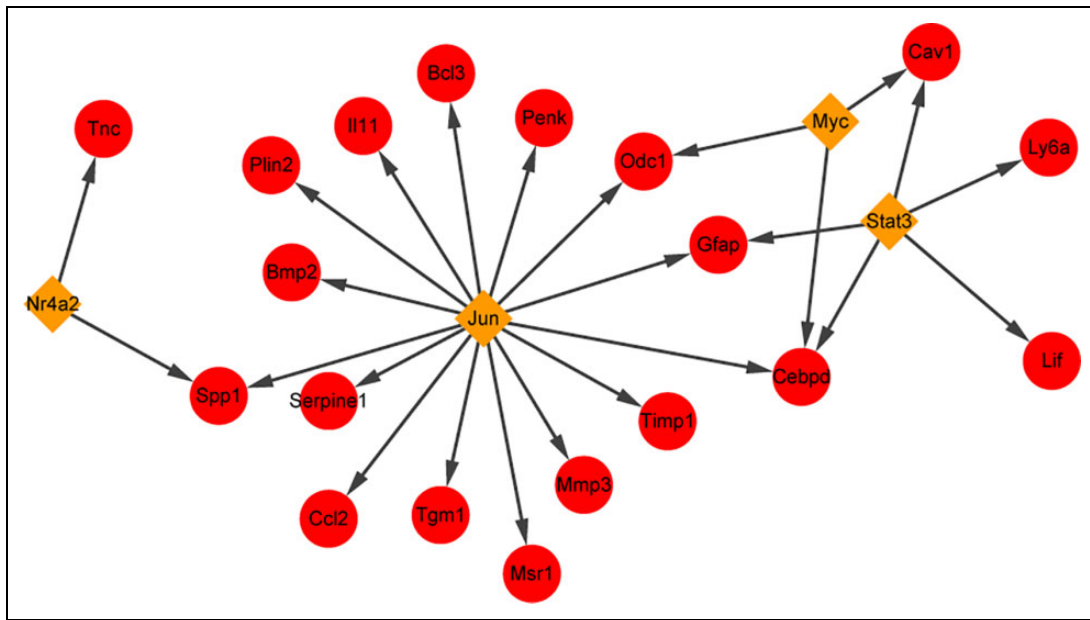
**Fig. 6.** Transcription factor-target regulatory network. The red circle indicates the uptrend gene, and the yellow diamond indicates the upregulated transcription factor.

(TIMP1), G protein subunit gamma 2 (GNG2), proenkephalin (PENK), cytoskeleton-associated protein 4 (CKAP4), complement C3a receptor 1 (C3AR1), glutamate metabotropic receptor 8 (GRM8), alpha-2-macroglobulin (A2M), which may be hub genes in PPI network.

PPI network was mined for functional modules. According to the threshold, five submodules were identified, as shown in Fig. 5A. KEGG pathway analysis of the five modules revealed that module 1 was involved in complement and coagulation cascades, module 2 was involved in endocytosis, module 3 was involved in neuroactive ligand–receptor interaction, module 4 was involved in phagosome, and module 5 was involved in ECM–receptor interaction (Fig. 5B). These findings indicated that the hub genes exhibited higher degrees and could serve critical roles in MTLE.

## TF-Target Regulatory Network Construction

Combined with the results of PPI network analysis, we are interested to further investigate the TF of DEGs. Four upregulated TFs, Jun proto-oncogene, AP-1 TF subunit (JUN), signal transducer and activator of transcription 3 (STAT3), nuclear receptor subfamily 4 group A member 2 (NR4A2), and myelocytomatosis oncogene (MYC), were obtained through TF analysis of the uptrend DEGs, in which JUN and Nr4a2 were significantly upregulated at 6 and 12 h compared with the control group, Myc was significantly upregulated at 12 and 24 h, and Stat3 was significantly upregulated at 24 h. Moreover, we found two TFs, JUN and NR4A2, that can regulate hub gene expression, including TIMP1, PENK, and TNC (Fig. 6).

## Upstream miRNA Prediction Analysis

A total of 26,834 miRNA–mRNA pairs were predicted, including 1014 miRNA and 465 target genes. We selected miRNAs with the top 20 target genes and constructed the miRNA-target network. As shown in Fig. 7A, 20 miRNAs, such as miR-240-3p, miR-298-5p, and miR-3473a and 317 target genes were included in the network. Pathway analysis showed that these miRNAs were significantly associated with HIF-1 signaling pathway, cAMP signaling pathway, calcium signaling pathway, and neuroactive ligand–receptor interaction (Fig. 7B, Supplemental Table S5).

## Expression and Survival Analysis of Key Genes in LGG Patients

To further investigate the relationship between MTLE and LGG, we selected 10 key genes with MTLE for survival analysis of LGG patients (Grade 2 and Grade 3) by the UALCAN database. Among these key genes, we found the expression levels of all key genes (C3, TIMP1, GNG2, CKAP4, PENK, TNC, JUN, STAT3, NR4A2, and MYC) were associated with poor overall survival of LGG patients ($P < 0.001$) (Fig. 8). However, the expression level of GNG2, PENK, NR4A2, and MYC did not have a significant difference between the LGG-Grade 2 and LGG-Grade 3 ($P > 0.05$) (Fig. 9). The comprehensive analysis has shown that a combination of 10 key genes of MTLE can predict the prognosis of LGG.
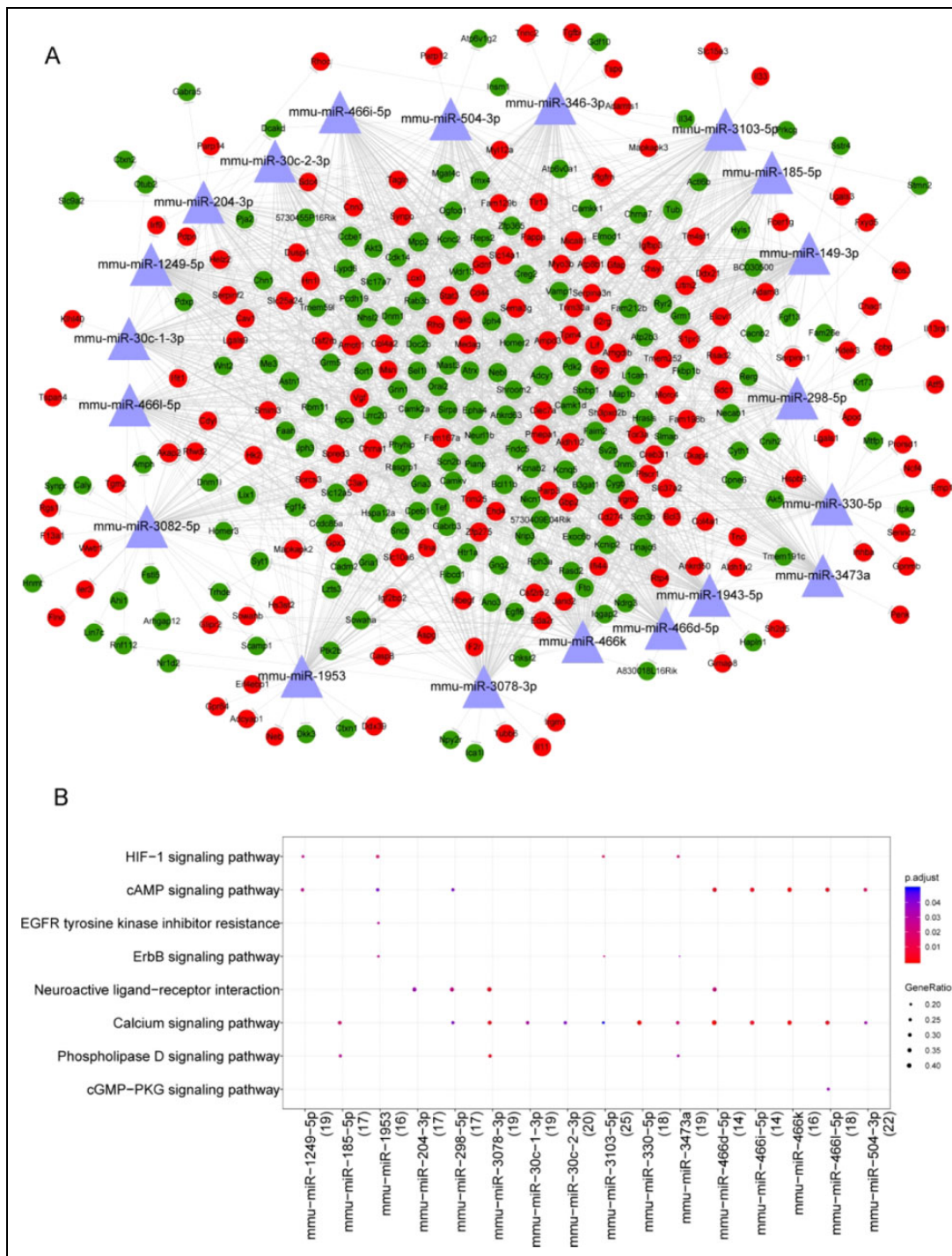
Fig. 7. miRNA-target regulatory network analysis. (A) miRNA-target regulatory network. The red circle indicates the uptrend gene, and the light purple triangle indicates the predicted miRNA. (B) Pathway analysis results of miRNAs. Color from blue to red indicates the decrease of adjusted *P*-value, and bubble size indicates the proportion of the number of enriched genes in the number of miRNA target genes annotated to KEGG pathway.

## qRT-PCR Verification

To confirm the results obtained from the microarray, some DEGs (Npas4, Atf3, Fosb, Fos, TIMP1, NR4A2, etc.) from three different time points (6, 12, and 24 h) as detected by qRT-PCR. Our findings suggested that majority of the investigated genes had congruent results between the microarray and qRT-PCR assays (Fig. 10). Primers for the DEGs were summarized in Supplemental Table S6.
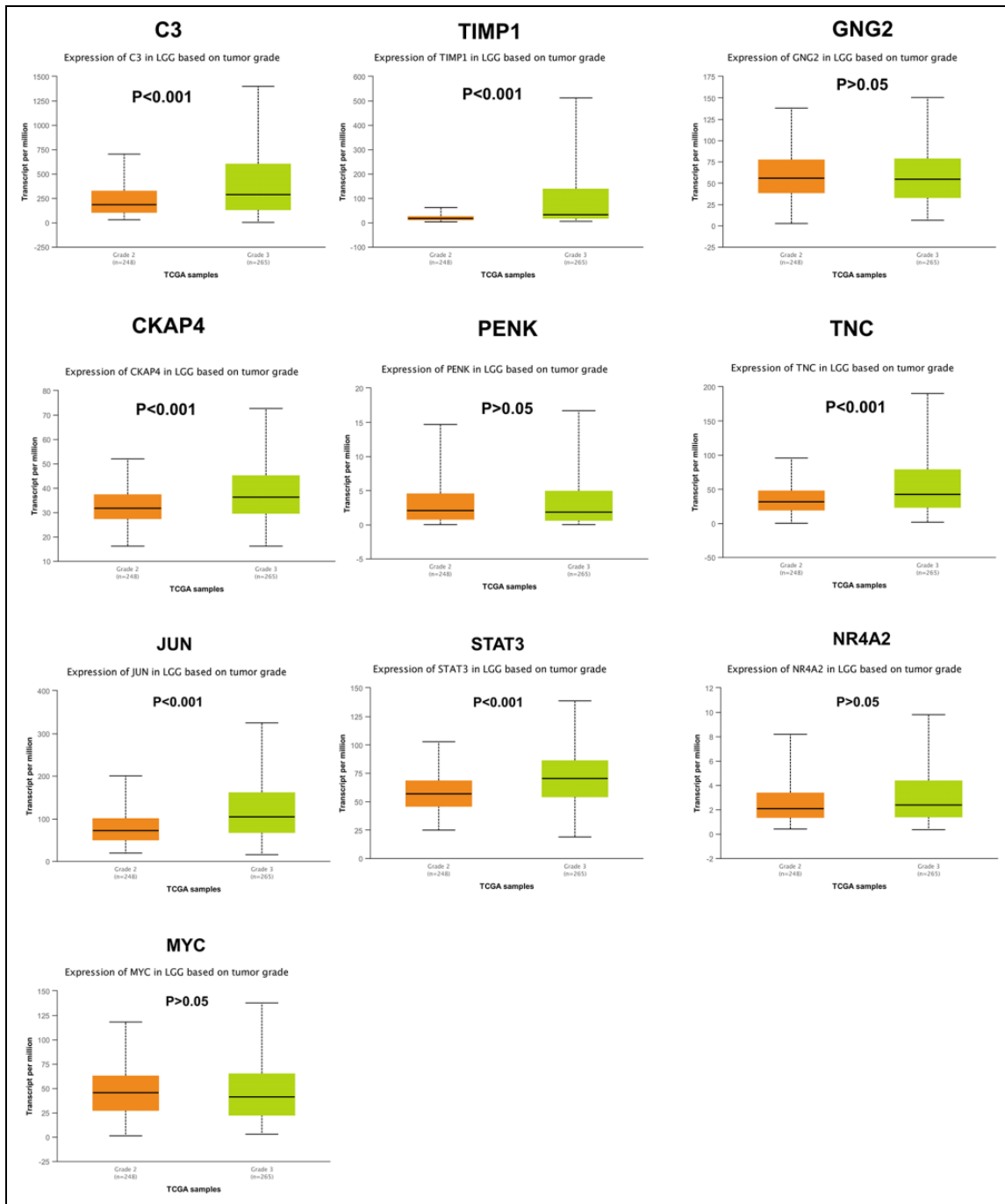
**Fig. 8.** Overall survival analysis of hub genes in brain LGG patients based on tumor grade. Survival analysis of C3, TIMP1, GNG2, CKAP4, PENK, TNC, JUN, STAT3, NR4A2, and MYC. *P* < 0.05 was considered to indicate a statistically significant difference. LGG: low-grade gliomas.

## Discussion

Bioinformatics analysis plays a crucial role in disease study, and it facilitates the understanding of disease processes by integrating data at the genome level with systematic bioinformatic methods. In this study, after time series clustering analysis of the DEGs, we identified 323 uptrend and 248 downtrend DEGs in MTLE and used a series of bioinformatics analyses to screen the key genes and pathways associated with MTLE. Moreover, these key genes are closely related to the prognosis of LGG.

Up- and downtrend DEGs lead to significant alterations in GO terms and KEGG pathways. The Biological Process (BP) of DEGs was abundantly enriched in the inflammatory
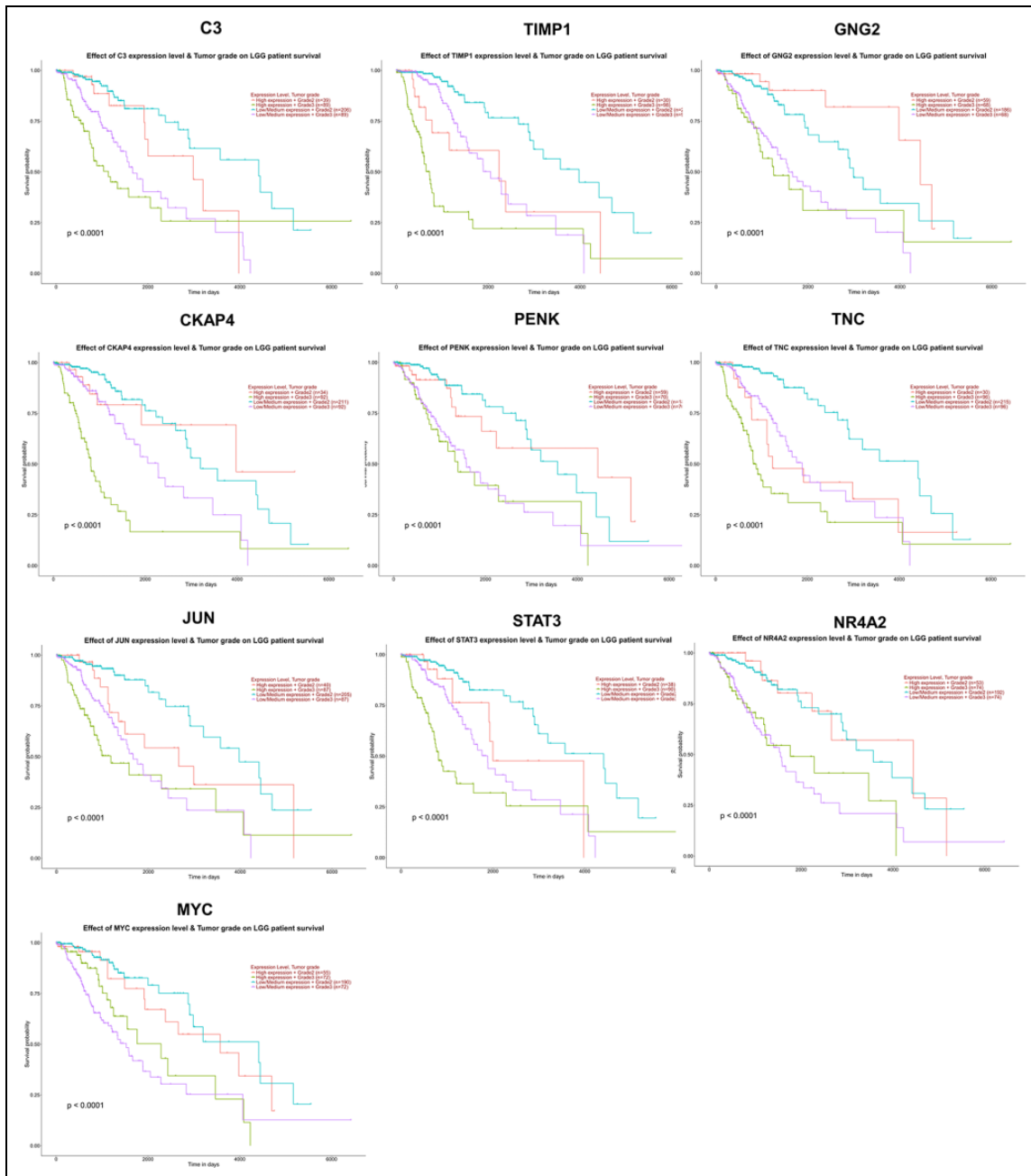
**Fig. 9.** Expression of hub genes in brain LGG patients based on tumor grade. Expression of C3, TIMP1, GNG2, CKAP4, PENK, TNC, JUN, STAT3, NR4A2, and MYC in LGG grade 2 and grade 3 patients. *P* < 0.05 was considered to indicate a statistically significant difference.

response, innate immune response, ion transport, chemical synaptic transmission, process. Previous studies have suggested inflammatory cells and molecules in the injured neuronal tissue are critical factors in the development of epilepsy[28-30]. The KEGG pathways are associated with cytokine–cytokine receptor interaction, JAK-STAT signaling pathway, TNF signaling pathway, calcium signaling pathway, and glutamatergic synapse. A recent study has revealed that the JAK-STAT and TNF signaling pathways may promote epileptogenesis[31,32], which is consistent with our findings.

Some hub genes, including C3, TIMP1, CKAP4, PENK, TNC, and GNG2, were identified based on PPI network of DEGs analyses. Additionally, several module genes, such as SYT1, KCNAB2, and COL4A2, were identified by MCODE. TF-hub genes regulatory network was also constructed to explore the molecular mechanism of MTLE progression. We identified four TFs, JUN, STAT3, NR4A2, and MYC, that can regulate the expression of these hub genes, which provide more evidence to illustrate the mechanisms in MTLE.
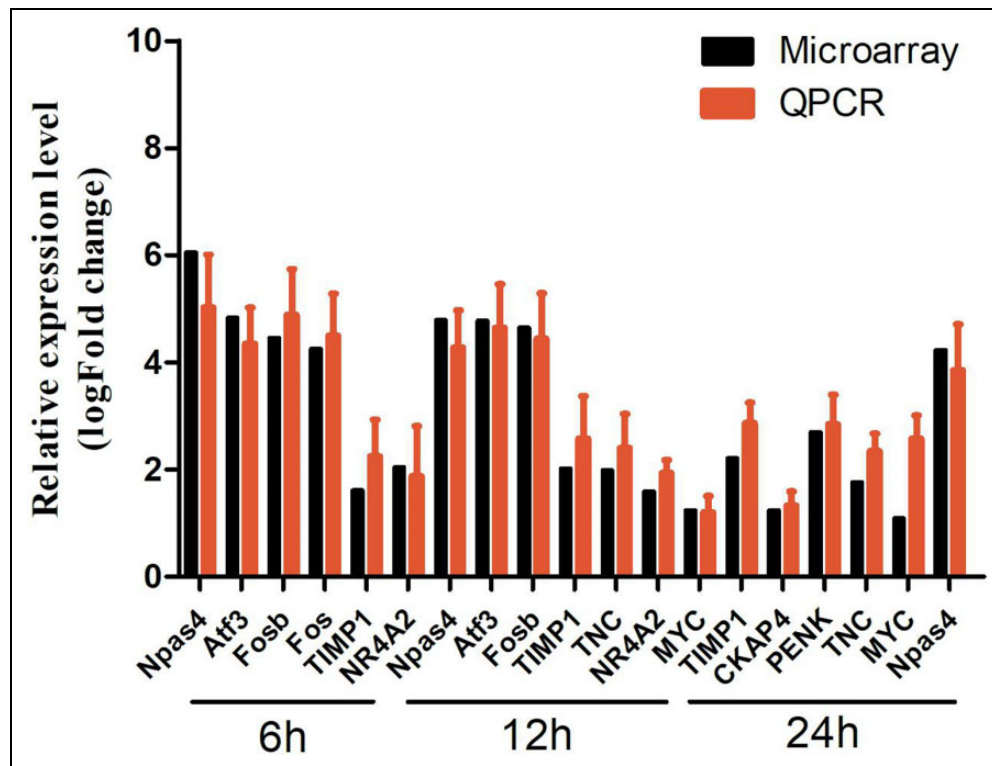
**Fig. 10.** The verification results of qRT-PCR. Npas4, Atf3, Fosb, Fos, TIMP1, and NR4A2 were upregulated at 6 h; Npas4, Atf3, Fosb, TIMP1, TNC, NR4A2, and MYC were upregulated at 12 h; TIMP1, CKAP4, PENK, TNC, MYC, and Npas4 were upregulated at 24 h. LogFC was calculated based on the mean intensity value from five mice by using the comparative Ct method and normalized to the housekeeping gene β-actin. FC: fold change; qRT-PCR: quantitative real-time polymerase chain reaction.

The study has reported that TLE is often related to granule cell dispersion, an abnormal broadening of the granule cell layer in the dentate gyrus. Functional inactivation of the extracellular matrix protein of Reelin is associated with the formation of granule cell dispersion[33]. TIMP1 is an endogenous inhibitor of a matrix metalloprotease and plays a central role in the control of Reelin cleavage. The epileptic conditions inhibit the activity of matrix metalloprotease by the upregulation of TIMP1[34]. In our study, TIMP1 was an uptrend gene, which was following the findings above. Thus, TIMP1 may serve as a therapeutic target in MTLE.

Moreover, we found that JUN, as an important TF, regulates the expression of TIMP1. JUN is one of the immediate early genes, which can be triggered by a range of pathologic insults to the brain, such as ischemia, trauma, and seizures[35,36]. Early upregulation of JUN transcription has been reported in hippocampal neurons of experimental seizures[37]. Lee et al.[38] also reported that the seizures were related to the expression of Jun in the hippocampal neurons, and the loss of hippocampal neurons was partly caused by cell apoptosis induced by Jun-mediated signaling pathway. We speculated that TF-JUN may play a role in MTLE by regulating TIMP1.

Moreover, PENK was also regulated by TF-JUN. Additionally, PENK was predicted to be regulated by miR-3473a.

Function analysis revealed that PENK was significantly enriched in GO terms of response to calcium ion (Supplemental Table S1). Interestingly, miR-3473a was also involved in the pathway of calcium signaling pathway. Voltage-gated calcium channels are widely expressed in the central nervous system of mammals. Changes in the expression and biophysical properties of voltage-gated calcium channels can easily lead to epilepsy[39]. The calcium ion is an important second messenger and plays a key role in normal brain function. It has been reported that calcium ion can regulate neuronal excitability, and intracellular calcium ion imbalance is a trigger for epilepsy[40]. Given the association of PENK with calcium ion as well as the involvement of its regulatory miRNA in calcium signaling pathway, we speculated that PENK may be associated with the occurrence of MTLE via calcium ion channels.

In addition to hub genes, several module genes may also be associated with MTLE, such as SYT1 (module 2), TNC (module 3), KCNAB2 (module 4), and COL4A2 (module 5). SYT1 encodes a synaptotagmin, which is depressed in the adult brain after seizure activity[41,42]. TNF protein was recently reported to be overexpressed in childhood with cortical dysplasia and epilepsy[43]. KCNAB2 is an ion channel gene and encodes a voltage-gated $K^+$ channel β-subunit protein. Lack of the β subunit decreased $K^+$ channel-

mediated membrane repolarization as well as increases the excitability of neurons. Thus, loss of KCNAB2 is associated with epilepsy[43]. Col4a2 encodes one of the six subunits of type IV collagen, mutations of which are associated with neurologic diseases, including epilepsy[44]. Taken together, we speculated that these module genes may act as biomarkers of MTLE.

Furthermore, survival analysis of UALCAN data indicated that C3, TIMP1, GNG2, CKAP4, PENK, TNC, JUN, STAT3, NR4A2, and MYC is associated with poorer overall survival of LGG patients. These findings indicated that the identified key genes could be clinical biomarkers in LGG. Consistent with our results, previous studies have revealed the overexpression of TIMP1 in old LGG patients[45]. The gene expression of complement C3 cells was regulated by interferon-γ and interleukin-1β in human astroglioma, which is correlated with the pathological stage[46]. Previous results suggest that TNC is not only a potential prognostic marker for GBM but also a potential marker for glioma cancer stem cells (CSCs)[47]. The comprehensive analysis showed that there was a certain correlation between MTLE and LGG, and the key genes of MTLE could be used to evaluate the potential prognostic value of survival in LGG patients.

In summary, we aimed to identify up- and downtrend DEGs by bioinformatics analysis to find key genes involved in the development of MTLE. Moreover, the study provides 10 useful DEGs for future investigation into the prognostic value of survival in LGG patients. However, further functional explorations are required to explore the functions of these DEGs in the progression of MTLE and LGG.

## Acknowledgments

## Author Contributions

All the authors contributed significantly to this article. AX conceived and supervised the study, JX and MS designed experiments, JG and YW carried out experiments, JX and AX wrote the manuscript.

## Data Availability

All datasets generated during the study are available on request from the corresponding author.

## Ethical Approval

Ethical Approval is not applicable for this article.

## Statement of Human and Animal Rights

This article does not contain any studies with human subjects. The data of animal subjects were obtained from the NCBI Gene Expression Omnibus[16] (GEO) database.

## Statement of Informed Consent

There are no human subjects in this article and informed consent is not applicable.

## Declaration of Conflicting Interests

The author(s) declared no potential conflicts of interest with respect to the research, authorship, and/or publication of this article.

## Funding

## ORCID iD

Jian Xu 🄳 https://orcid.org/0000-0002-3087-824X

## Supplemental Material

Supplemental material for this article is available online.

## References

1. Devinsky O, Vezzani A, O'Brien TJ, Jette N, Scheffer IE, de Curtis M, Perucca P. Epilepsy. Nat Rev Dis Primers. 2018;4: 18024.

2. Geller EB, Skarpaas TL, Gross RE, Goodman RR, Barkley GL, Bazil CW, Berg MJ, Bergey GK, Cash SS, Cole AJ. Brain-responsive neurostimulation in patients with medically intractable mesial temporal lobe epilepsy. Epilepsia. 2017;58(6): 994–1004.

3. Frauscher B, von Ellenrieder N, Dubeau F, Gotman J. Different seizure-onset patterns in mesiotemporal lobe epilepsy have a distinct interictal signature. Clin Neurophysiol. 2017;128(7): 1282–1289.

4. Orsini A, Zara F, Striano P. Recent advances in epilepsy genetics. Neurosci Lett. 2018;667:4–9.

5. Consortium TILAE. Genetic determinants of common epilepsies: a meta-analysis of genome-wide association studies. Lancet Neurol. 2014;13(9):893–903.

6. Consortium TILAE. Genome-wide mega-analysis identifies 16 loci and highlights diverse biological mechanisms in the common epilepsies. Nat Commun. 2018;9(1):5269.

7. Gorter JA, van Vliet EA, Aronica E, Breit T, Rauwerda H, da Silva FHL, Wadman WJ. Potential new antiepileptogenic targets indicated by microarray analysis in a rat model for temporal lobe epilepsy. J Neurosci. 2006;26(43):11083–11110.

8. Sharma AK, Searfoss GH, Reams RY, Jordan WH, Snyder PW, Chiang AY, Jolly RA, Ryan TP. Kainic acid-induced F-344 rat model of mesial temporal lobe epilepsy: gene expression and canonical pathways. Toxicol Pathol. 2009;37(6): 776–789.

9. Vieira A, De Matos A, Do Canto A, Rocha C, Carvalho B, Pascoal V, Norwood B, Bauer S, Rosenow F, Gilioli R. RNA sequencing reveals region-specific molecular mechanisms

associated with epileptogenesis in a model of classical hippocampal sclerosis. Sci Rep. 2016;6(1):1–10.

10. Ben-Ari Y, Tremblay E, Ottersen O. Injections of kainic acid into the amygdaloid complex of the rat: an electrographic, clinical and histological study in relation to the pathology of epilepsy. Neuroscience. 1980;5(3):515–528.

11. Guillemain I, Kahane P, Depaulis A. Animal models to study aetiopathology of epilepsy: what are the features to model? Epileptic Disord. 2012;14(3):217–225.

12. Motti D, Le Duigou C, Eugène E, Chemaly N, Wittner L, Lazarevic D, Krmac H, Marstrand T, Valen E, Sanges R. Gene expression analysis of the emergence of epileptiform activity after focal injection of kainic acid into mouse hippocampus. Eur J Neurosci. 2010;32(8):1364–1379.

13. Kalozoumi G, Kel-Margoulis O, Vafiadaki E, Greenberg D, Bernard H, Soreq H, Depaulis A, Sanoudou D. Glial responses during epileptogenesis in Mus musculus point to potential therapeutic targets. PLoS One. 2018;13(8):e0201742.

14. Gonzalez Castro LN, Milligan TA. Seizures in patients with cancer. Cancer. 2020;126(7):1379–1389.

15. Xu Y, Geng R, Yuan F, Sun Q, Liu B, Chen Q. Identification of differentially expressed key genes between glioblastoma and low-grade glioma by bioinformatics analysis. Peer J. 2019;7: e6560.

16. Barrett T, Suzek TO, Troup DB, Wilhite SE, Ngau W-C, Ledoux P, Rudnev D, Lash AE, Fujibuchi W, Edgar R. NCBI GEO: mining millions of expression profiles—database and tools. Nucleic Acids Res. 2005;33(suppl 1):D562–D566.

17. Smyth GK.limma: Linear Models for Microarray Data. In: Gentleman R, Carey VJ, Huber W, Irizarry RA, Dudoit S, eds. Bioinformatics and Computational Biology Solutions Using R and Bioconductor. New York (NY): Springer; 2005:397–420.

18. Ernst J, Bar-Joseph Z. STEM: a tool for the analysis of short time series gene expression data. BMC Bioinformatics. 2006; 7(1):191.

19. Ashburner M, Ball CA, Blake JA, Botstein D, Butler H, Cherry JM, Davis AP, Dolinski K, Dwight SS, Eppig JT, Harris MA, et al. Gene Ontology: tool for the unification of biology. Nat Genet. 2000;25(1):25–29.

20. Kanehisa M, Goto S. KEGG: kyoto encyclopedia of genes and genomes. Nucleic Acids Research. 2000;28(1):27–30.

21. Szklarczyk D, Franceschini A, Wyder S, Forslund K, Heller D, Huerta-Cepas J, Simonovic M, Roth A, Santos A, Tsafou KP. STRING v10: protein–protein interaction networks, integrated over the tree of life. Nucl Acids Res. 2014;43(D1):D447–D52.

22. Shannon P, Markiel A, Ozier O, Baliga N, Wang J, Ramage D, Amin N, Schwikowski B, Ideker T. Cytoscape: a software environment for integrated models of biomolecular interaction networks. Genome Res. 2003;13(11):2498–2504.

23. Yu Tang ML, Jianxin Wang, Yi Pan, Fang-Xiang Wu. CytoNCA: a cytoscape plugin for centrality analysis and evaluation of biological networks. Biosystems. 2015;127:67–72.

24. Bader GD, Hogue CWV. An automated method for finding molecular complexes in large protein interaction networks. BMC Bioinformatics. 2003;4:2.

25. Yu G, Wang L-G, Han Y, He Q-Y. clusterProfiler: an R Package for comparing biological themes among gene clusters. OMICS. 2012;16(5):284–287.

26. Han H, Cho J-W, Lee S, Yun A, Kim H, Bae D, Yang S, Kim CY, Lee M, Kim E. TRRUST v2: an expanded reference database of human and mouse transcriptional regulatory interactions. Nucleic Acids Res. 2018;46(D1):D380–D386.

27. Dweep H, Gretz N. miRWalk2. 0: a comprehensive atlas of microRNA-target interactions. Nat Methods. 2015;12(8): 697–697.

28. Rana A, Musto AE. The role of inflammation in the development of epilepsy. J Neuroinflammation. 2018;15(1):144.

29. Alyu F, Dikmen M. Inflammatory aspects of epileptogenesis: contribution of molecular inflammatory mechanisms. Acta Neuropsychiatr. 2017;29(1):1–16.

30. Guo XQ, Cao YL, Hao F, Yan ZR, Wang ML, Liu XW. Tangeretin alters neuronal apoptosis and ameliorates the severity of seizures in experimental epilepsy-induced rats by modulating apoptotic protein expressions, regulating matrix metalloproteinases, and activating the PI3K/Akt cell survival pathway. Adv Med Sci. 2017;62(2):246–253.

31. Patel DC, Wallis G, Dahle EJ, McElroy PB, Thomson KE, Tesi RJ, Szymkowski DE, West PJ, Smeal RM, Patel M, Fujinami RS, et al. Hippocampal TNFalpha signaling contributes to seizure generation in an infection-induced mouse model of limbic epilepsy. eNeuro. 2017;4(2):ENEURO.0105-17.2017.

32. Han CL, Ge M, Liu YP, Zhao XM, Wang KL, Chen N, Meng WJ, Hu W, Zhang JG, Li L, Meng FG. LncRNA H19 contributes to hippocampal glial cell activation via JAK/STAT signaling in a rat model of temporal lobe epilepsy. J Neuroinflammation. 2018;15(1):103.

33. Orcinha C, Münzner G, Gerlach J, Kilias A, Follo M, Egert U, Haas CA. Seizure-induced motility of differentiated dentate granule cells is prevented by the central Reelin fragment. Front Cell Neurosci. 2016;10:183.

34. Tinnes S, Ringwald J, Haas CA. TIMP-1 inhibits the proteolytic processing of Reelin in experimental epilepsy. FASEB J. 2013;27(7):2542–2552.

35. Li D, Wu J, Luo L, Qiao L, Liu Z, Lu G, Wang Y. Role of c-Jun N-terminal kinase-mediated FOXO3a nuclear translocation in neuronal apoptosis in neonatal rats with hypoxic-ischemic brain damage [in Chinese]. Zhongguo Dang Dai Er Ke Za Zhi. 2017;19(4):458–462.

36. Rehman SU, Ahmad A, Yoon G-H, Khan M, Abid MN, Kim MO. Inhibition of c-Jun N-terminal kinase protects against brain damage and improves learning and memory after traumatic brain injury in adult mice. Cereb Cortex. 2018;28(8):2854–2872.

37. Lee JK, Kang SS, Lee MC. Stress protein expression in kainate-induced experimental temporal lobe epilepsy in rats. J Korean Neurosurg Soc. 1998;27(12):1641.

38. Lee MC, Rho JL, Kim MK, Woo YJ, Kim JH, Nam SC, Suh JJ, Chung WK, Moon JD, Kim HI. c-JUN expression and apoptotic cell death in kainate-induced temporal lobe epilepsy. J Korean Med Sci. 2001;16(5):649–656.

39. Rajakulendran S, Hanna MG. The role of calcium channels in epilepsy. Cold Spring Harbor Perspect Med. 2016;6(1):a022723.

40. Xu J-H, Tang F-R. Voltage-dependent calcium channels, calcium binding proteins, and their interaction in the pathological process of epilepsy. Int J Mol Sci. 2018;19(9):2735.

41. Tocco G, Bi X, Vician L, Lim IK, Herschman H, Baudry M. Two synaptotagmin genes, Syt1 and Syt4, are differentially regulated in adult brain and during postnatal development following kainic acid-induced seizures. Brain Res Mol Brain Res. 1996;40(2):229–239.

42. Baker K, Gordon SL, Melland H, Bumbak F, Scott DJ, Jiang TJ, Owen D, Turner BJ, Boyd SG, Rossi M. SYT1-associated neurodevelopmental disorder: a case series. Brain. 2018; 141(9):2576–2591.

43. Qin L, Liu X, Liu S, Liu Y, Yang Y, Yang H, Chen Y, Chen L. Differentially expressed proteins underlying childhood cortical dysplasia with epilepsy identified by iTRAQ proteomic profiling. Plos One. 2017;12(2):e0172214.

44. Körber I, Kudernatsch M, Hartlieb T, Kirschner C, Coras R, Blümcke I, Winkler P, Staudt M, Berweck S, Kluger G. Clinical course, epilepsy surgery and outcome in pediatric patients with COL4A1/COL4A2 associated epilepsy. Neuropediatrics. 2019;50(S 02):S1–S55.

45. Wang H, Wang X, Xu L, Zhang J, Cao H. Prognostic significance of age related genes in patients with lower grade glioma. J Cancer. 2020;11(13):3986–3999.

46. Barnum SR, Jones JL. Differential regulation of C3 gene expression in human astroglioma cells by interferon-gamma and interleukin-1 beta. Neurosci Lett. 1995; 197(2):121–124.

47. Nie S, Gurrea M, Zhu J, Thakolwiboon S, Heth JA, Muraszko KM, Fan X, Lubman DM. Tenascin-C: a novel candidate marker for cancer stem cells in glioblastoma identified by tissue microarrays. J Proteome Res. 2015;14(2):814–822.